Alignment of the CMS silicon tracker

Tapio Lampén (on behalf of the CMS Collaboration)
Helsinki Institute of Physics, P.O. Box 64, Fin-00014 Helsinki, Finland
E-mail: tapio.lampen@cern.ch

Abstract. The CMS all-silicon tracker consists of 16 588 modules, embedded in a solenoidal magnet providing a field of B = 3.8 T. The targeted performance requires that the software alignment tools determine the module positions with a precision of a few micrometers. Ultimate local precision is reached by the determination of sensor curvatures, challenging the algorithms to determine about 200 000 parameters simultaneously. The main remaining challenge for alignment are the global distortions that systematically bias the track parameters and thus physics measurements. They are controlled by adding further information into the alignment work-flow, e.g. the mass of decaying resonances or track data taken with B = 0 T. To make use of the latter and also to integrate the determination of the Lorentz angle into the alignment procedure, the alignment framework has been extended to treat position sensitive calibration parameters. This is relevant since due to the increased LHC luminosity in 2012, the Lorentz angle exhibits time dependence. Cooling failures and ramping of the magnet can induce movements of large detector sub-structures. These movements are now detected in the CMS prompt calibration loop to make the corrections available for the reconstruction of the data for physics analysis. The geometries are finally carefully validated. The monitored quantities include the basic track quantities for tracks from both collisions and cosmic ray muons and physics observables.

1. Introduction

The central feature of the Compact Muon Solenoid (CMS) apparatus is a superconducting solenoid of 6 m internal diameter. Within the superconducting solenoid volume are a silicon pixel and strip tracker, a lead tungstate crystal electromagnetic calorimeter (ECAL), and a brass/scintillator hadron calorimeter (HCAL). Muons are measured in gas-ionization detectors embedded in the steel return yoke outside the solenoid. Extensive forward calorimetry complements the coverage provided by the barrel and endcap detectors.

CMS uses a right-handed coordinate system, with the origin at the nominal interaction point, the x axis pointing to the centre of the LHC, the y axis pointing up (perpendicular to the LHC plane), and the z axis along the anticlockwise-beam direction. The polar angle θ is measured from the positive z axis and the azimuthal angle ϕ is measured in the x-y plane. Muons are measured in the pseudorapidity range $|\eta| < 2.4$, with detection planes made using three technologies: drift tubes, cathode strip chambers, and resistive plate chambers. Matching muons to tracks measured in the silicon tracker results in a transverse momentum resolution between 1 and 5%, for p_T values up to 1 TeV.

The inner tracker measures charged particles within the pseudorapidity range $|\eta| < 2.5$. It consists of 1 440 silicon pixel and 15 148 silicon strip detector modules and is located in the 3.8 T

field of the superconducting solenoid. It provides an impact parameter resolution of $\sim$15 μm and a transverse momentum p_T resolution of about 1.5% for 100 GeV particles.

The CMS apparatus has an overall length of 22 m, a diameter of 15 m, and weighs 14 000 t. A more detailed description can be found in [1].

To fully exploit the single hit resolution of 9 μm for pixel and of 23–60 μm for strip sensors, the positions of the sensors must be known to a precision of a few micrometers. This can be best achieved with track-based alignment algorithms. For the CMS tracker these have been applied using tracks from cosmic ray events [2], adding tracks from first LHC collisions [3], and from data taking periods of 2010–2012 [4, 5]. The alignment process has improved during the years, and new features have been added.

The track-based alignment algorithms aim to minimize the χ^2 function, in which the sum of squares of track-hit residuals is collected over a large number of tracks and sensors. The minimization is carried out with respect to selected degrees of freedom (DoF) of each sensor corresponding to its translation, rotation and shape [5]. However, for those sensors which are sensitive only in one coordinate, it is not meaningful to use all these DoFs.

Details of the minimization process can be found in [6, 7] and [8] for the Millepede II and H.I.P. approaches, both used in CMS.

This article gives an overview of the track-based alignment process of the CMS silicon tracker and presents the main improvements and results in 2012, followed by a summary.

2. Alignment in CMS in 2012

The **full-scale alignment** of the CMS silicon tracker consists of alignment of all individual sensors for all their reasonable degrees of freedom (DoF)[1]: 9 DoFs for pixel modules and 8 DoFs for strip sensors (sensitive only in one coordinate). In addition, larger groups of sensors corresponding to physical structures of CMS can be aligned for 9 DoFs. Redundant DoFs are avoided with use of **hierarchy constraints** [2]. This allows good control for time-dependent effects, which typically influence structures larger than individual sensors, for which the alignment compared to nearby sensors is rather stable in time. Therefore, when full-scale alignment parameters are defined with a large dataset, the alignment parameters of large structures can be allowed to vary with time.

The alignment of **high-level structures** is an approach in which frames of modules, layers or even subdetectors (such as the pixel detector) are aligned instead of their components. This approach requires less tracks and is faster to carry out, and is fully sufficient, when a full-scale alignment has previously been carried out, and when there is no reason to suspect deterioration in the sensor-level alignment parameters.

In 2012, new alignments were applied twice in the prompt reconstruction. First, at the beginning of the year, a high-level structure alignment was performed with cosmic ray muon data recorded while there were no collisions provided by the LHC. Later a high-level structure alignment was again carried out together with a pixel module-level alignment taking into account an update in the Lorentz angle calibrations.

In the re-reconstruction of the 2012 data, new alignment parameters were used three times. The main motivation was improvements achieved in the Lorentz angle calibrations.

3. Improvements in Alignment in 2012

Important improvements in the alignment process have been introduced during the past years, especially starting from 2010 and 2011 when abundant amount of high-quality tracks with high momentum became available.

[1] The possible degrees of freedom for alignment are three translational DoFs, three rotational DoFs, and three DoFs corresponding to Legendre polynomials parametrising the deviations from an ideal plane [5].

The following improvements [5] were introduced in 2011, and were thus ready to be used in the data taking of 2012:

- parametrization of sensor shapes;
- consideration of effects of multiple scattering in the track model used in determination of alignment parameters;
- for $Z^0 \to \mu^+\mu^-$ events: use of the mass of the Z^0 boson as a constraint (in the form of a penalty function to the χ^2 function), together with a vertex constraint enforcing the muons to emerge from a common vertex (described in more detail in [5]); and
- monitoring of time dependence of large structures of the pixel detector.

3.1. Parametrization of sensor shapes

The possibility to model the shape of the sensors with second-order Legendre polynomials has been introduced to the alignment process [5]. Also, the angles and offsets between two daisy-chained sensors in the modules in the outer tracker can be corrected in the alignment.

During construction, the planarity tolerance for the strip sensors was 100 μm [1]. This kind of deviation would create a bias in the measurement direction u of the sensor, depending on the angle ψ of the track with respect to the normal of the sensors as $\Delta u = \Delta w * \tan\psi$, where Δw is the deviation from the ideal plane at the impact point. This is depicted in figure 1. With the same equation, the Δw and thus the shape can be scanned over the sensor surface.

The bias resulting from non-planar sensors is especially large for sensors of the innermost layer of the pixel barrel. At the edge of the 66 mm wide modules, this bias can be of the order of 100 μm.

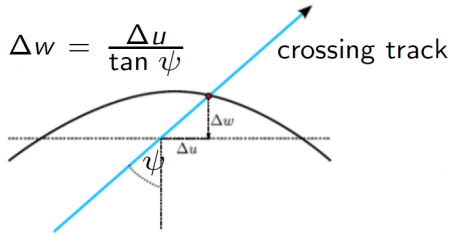

Figure 1. Illustration of a bias Δu in the measurement direction caused by the non-planar shape of a sensor. The sensor differs from the ideal plane by Δw at the crossing point. The angle between the track and the normal of the ideal sensor surface is ψ. The bow is largely exaggerated.

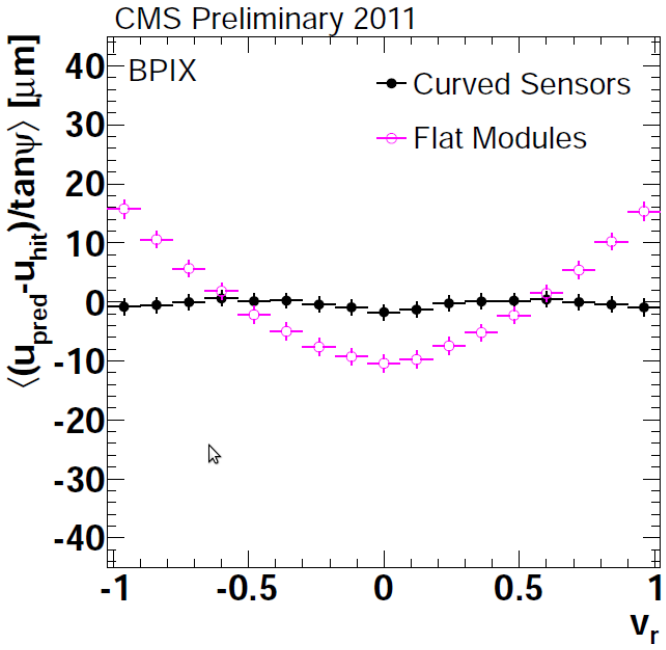

Figure 2. Sensor bow (Δw) as function of the normalized measurement direction v_r, where values of ± 1 correspond to the edges of the sensor.

When the sensor shape parameters are taken into account in hit reconstruction, the related bias is practically corrected. This is illustrated in figure 2, which presents Δw over the normalized

relative local track coordinate v_r (corresponding to the global z direction) averaged over pixel barrel sensors. The purple open circles ("Flat Modules") correspond to a situation in which no sensor shape parameters are applied, and average deviation of the order of 10–20 μm can be seen. The black filled circles ("Curved sensors") correspond to the situation when these parameters are used, and the deviations are below 5 μm of absolute value.

3.2. Weak modes and mass constraints

Alignment with the minimization of the χ^2 of track-hit residuals is an efficient way to correct for the uncorrelated sensor misalignments and in this way to improve the precision of measurements and physics variables. A more difficult type of misalignments are, however, those correlated distortions, which do not affect or affect very little the χ^2 function (the "weak modes"). A set of nine basic weak modes and their implication on physics analyses is studied in [4].

Weak modes can be constrained in alignment by using tracks corresponding to multiple topologies (collision tracks with vertices from a wide area, tracks from cosmic rays, etc.). In addition, mass constraints for well-known resonances can be used. For instance, use of cosmic ray tracks is an efficient way to constrain the **telescope weak mode** ($\Delta z \sim r$), which creates a bias in the measured η value of the track.

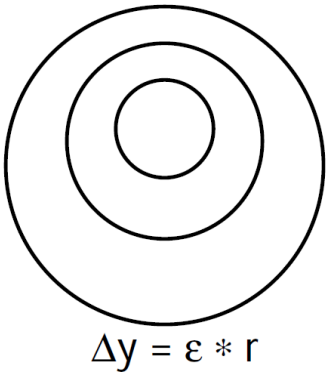

Figure 3. Illustration of the Sagitta weak mode. Individual sensors are not shown, only the layers they are attached to. In this correlated distortion, layers are shifted vertically (Δy) by an amount proportional to their radial coordinate r.

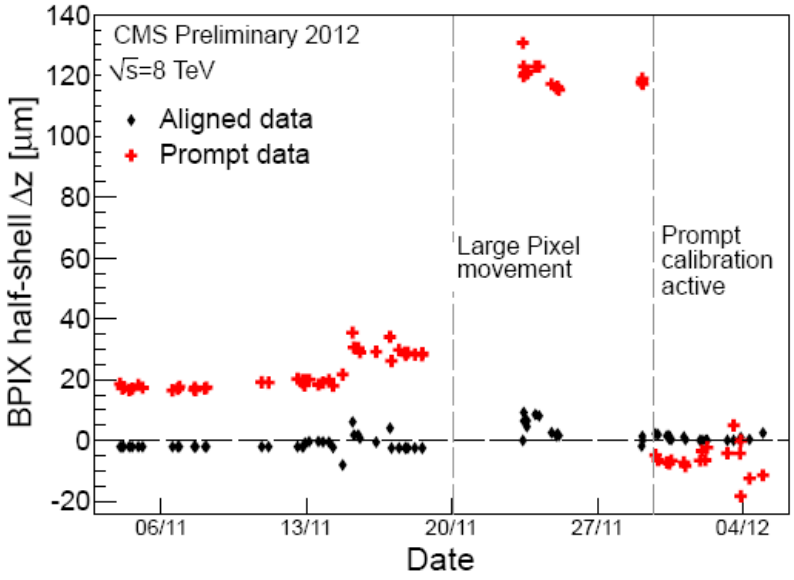

Figure 4. Relative misalignment Δz of the two pixel half barrels along the beam line Δz as function of date in November-December 2012. A 100 μm movement appears on November 22nd, and is corrected with the PCL a week later.

In 2011, a variation of the Z^0 mass as function of the ϕ angle of the positively charged muon from $Z^0 \to \mu^+\mu^-$ decays was observed. This **ϕ-dependent curvature bias** was suspected to be caused by a **sagitta weak mode**, in which sensors are displaced as $\Delta y \sim r$, as shown in figure 3. This systematic distortion can bias the track curvature, which is inversely proportional to the transverse momentum: $\kappa \sim 1/p_T$. It was studied with $Z^0 \to \mu^+\mu^-$ events, which can be used to reveal this bias in the following way. The fitted[2] invariant mass of Z^0 is presented as

[2] The invariant mass distribution is fitted with a wide fit in the range 75–105 GeV/c^2 and the Z width is set to the PDF value of 2.495 GeV/c^2. In the fit, a Breit-Wigner function convoluted with a Crystal ball function is used (it models finite track resolution and radiative tail) summed with an exponential background.

function of the muon direction, separating μ^+ and μ^-. A sinusoidal dependency can reveal the existence of a sagitta weak mode. The result is shown in figure 5 with respect to the ϕ angle, and in figure 6 with respect to the η angle [3]. In 2012, the ϕ dependence of the curvature bias has decreased as a result of applying substantial weights to the $Z^0 \to \mu^+\mu^-$ events in alignment.

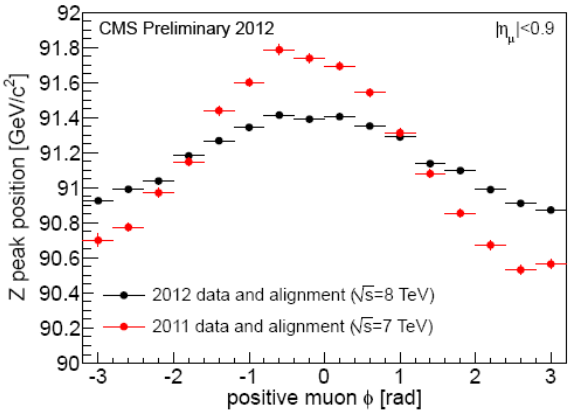

Figure 5. Reconstructed mass for $Z^0 \to \mu^+\mu^-$ decays as a function of ϕ of the μ^+. Results for 2011 data and alignment are shown in red, and those for 2012 in black.

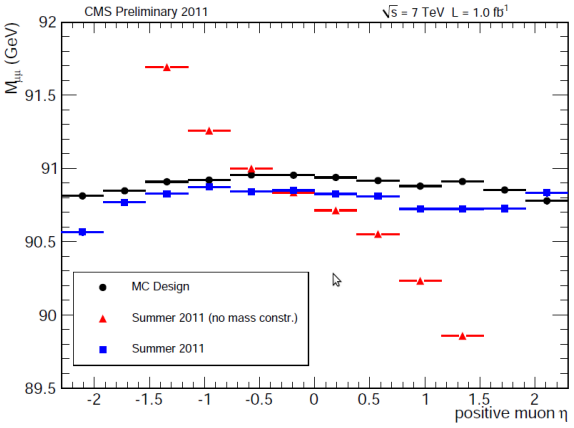

Figure 6. Reconstructed mass for $Z^0 \to \mu^+\mu^-$ decays as a function of η of the μ^+. Results with perfect alignment and simulated events are shown with black circles. Results with and without the mass-constrained Z events used in alignment are shown with blue squares and red triangles, respectively, for data from 2011.

3.3. Prompt calibration loop

In CMS, the **prompt calibration loop** (PCL) is a data stream, in which some measured data is immediately reconstructed for purposes of data quality monitoring, alignment and calibration. With these data, the offline conditions database can be updated so that the actual physics data stream from CMS can be reconstructed after a short, intentional delay with up-to-date conditions.

At the end of 2012, the PCL was able to calculate 6 alignment parameters for the pixel half barrels. It could provide feedback well within the time limit of 48 hours, after which data from the same run was reconstructed and made available to physics analyses.

During the last month of proton-proton collisions of 2012, the PCL was running for monitoring purposes, and thus not used in updating alignment parameters. A major relative movement of the pixel half-shells along the z coordinate was detected on November 22nd. The PCL was activated on November 30th to recover this movement, which later was diagnosed to be caused by a cooling failure. These movements are shown in figure 4, which depicts with red crosses the relative z-shift of the half-shells with the track-vertex residuals as a function of date. The black diamonds refer to the situation when this movement has been corrected for later in re-reconstruction.

[3] This result does not illustrate CMS muon reconstruction and calibration performance. Additional momentum calibration is applied in addition when necessary.

3.4. Lorentz angle calibration

A possibility to calibrate the Lorentz angle has also been implemented in the Millepede II alignment procedure in 2012. As shown in figure 7, in presence of a magnetic field, the Lorentz force deflects drifting signal charge by the Lorentz angle. This effect causes shift of the measured hit positions in the local u direction by $\Delta u = \tan(\theta_{LA}) * d/2$, where θ_{LA} is the Lorentz angle, and d is the width of the sensor.

To calibrate the Lorentz angle (LA), tracks recorded both with magnetic field on and off are needed to disentangle LA effects from genuine misalignments. The full 2012 data with 60 million tracks were used: tracks of isolated muons, $Z^0 \rightarrow \mu^+\mu^-$ events, cosmic ray muons (at both 0 T and 3.8 T), low p_T tracks and collision tracks recorded at 0 T. The Lorentz angle was calibrated for the pixel detector with a granularity of 65 periods of time (of 2012). In addition, 24 spatial parameters were used: three corresponding to the cylindrical layers of the pixel barrel surrounding the interaction point (at radii of 4.4, 7.3 and 10.2 cm [1]), and 8 corresponding to rings in each layer (sensors on one layer with the same z coordinate). This leads to 1560 additional parameters for the alignment procedure.

The Lorentz angle development for all layers (on ring 4) of the pixel barrel is shown in figure 8 as function of integrated luminosity collected by CMS during 2012. The development for layers 1,2 and 3 are shown in figures 9, 10, and 11, respectively. The following observations can be made:

- evolution of the Lorentz angle is consistent in all rings within each layer;
- there is a significant offset of the Lorentz angle values for negative and positive halves of the pixel barrel along Z (rings 1–4 compared to rings 5–8);
- behaviour of the Lorentz angle seems to be different for different layers; it is however suspected that this is caused by different radiation doses, and can follow the same behaviour delayed with time; and
- the largest change of the Lorentz angle (layer 1, ring 4) through whole 2012 is equivalent to the shift of the modules by up to 4 μm.

The offset seen between Lorentz angles in rings 1–4 and 5–8 is suspected to be caused by a difference in their grounding, which generates a difference in the bias voltage of the sensors. This hypothesis will be verified when data taking restarts.

In 2012, the effect caused by the time-dependent changes of the Lorentz angle is only of the size of a few μm, but this issue will certainly be relevant in 2015, when increased LHC luminosity and the intense radiation will generate time-dependency in the Lorentz angle calibration.

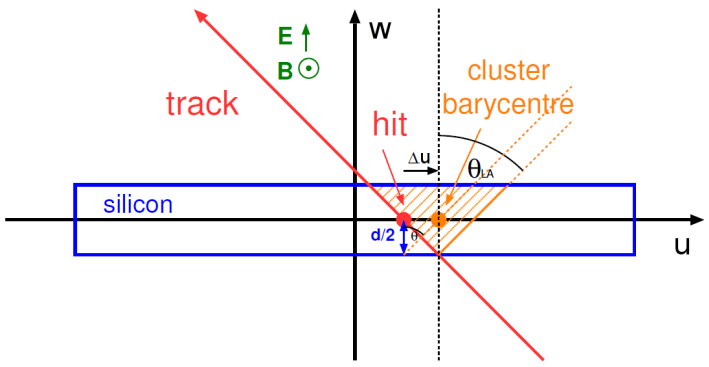

Figure 7. Illustration of the Lorentz angle. Due to the magnetic field, charge carriers in the silicon drift to the direction indicated by orange lines, with an angle with the electric field lines called the Lorentz angle. As a result, the cluster barycentre is reconstructed in a biased position, unless the Lorentz effect is properly accounted for.

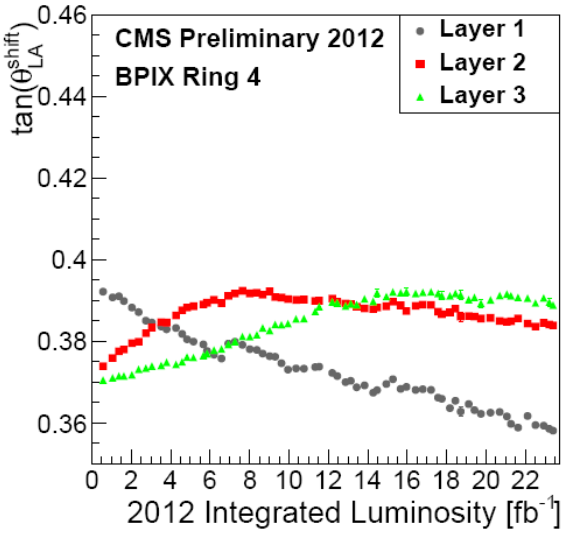

Figure 8. Evolution of the Lorentz angle in 2012 for innermost sensors (ring 4) of all three pixel barrel layers.

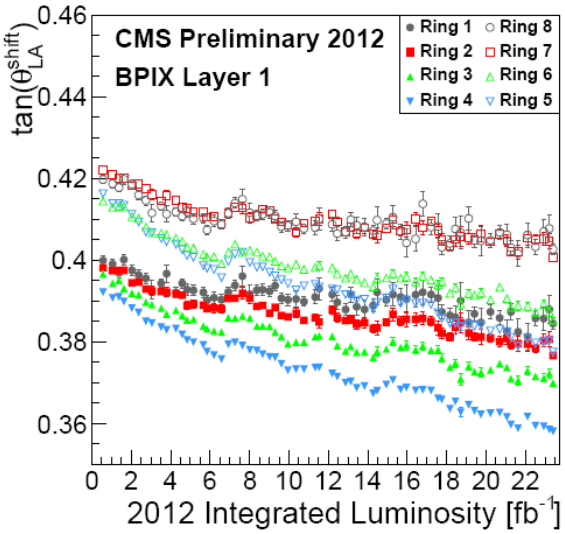

Figure 9. Evolution of the Lorentz angle in 2012 for 8 rings of layer 1 of the pixel barrel.

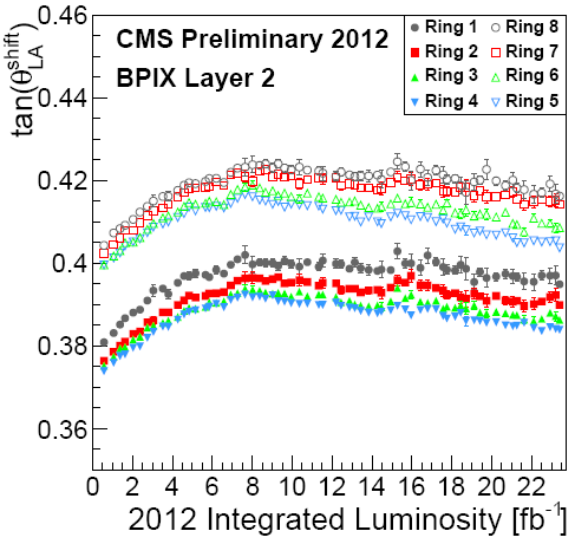

Figure 10. Evolution of the Lorentz angle in 2012 for 8 rings of layer 2 of the pixel barrel.

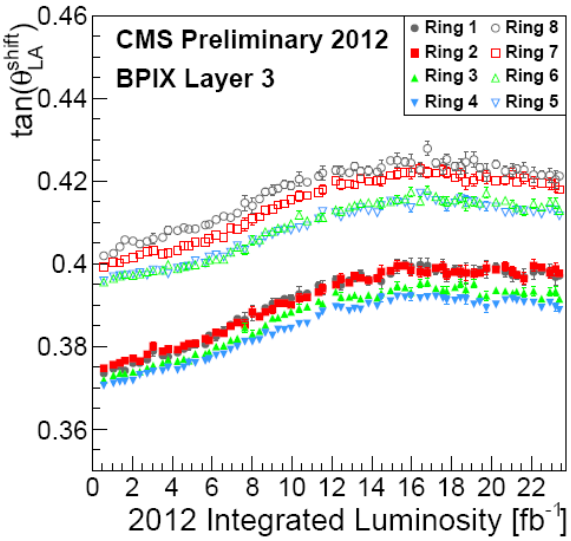

Figure 11. Evolution of the Lorentz angle in 2012 for 8 rings of layer 3 of the pixel barrel.

4. Summary

Alignment of the CMS silicon tracker has been routinely performed with the Millepede II algorithm calibrating 200 000 alignment parameters. The alignment work-flow provides quick response to data taking with a run-by-run alignment of large structures. The improvements in 2012 consist of: calibration of sensor shape parameters, alignment calibration operational in the prompt calibration loop, reduction of amplitude of the ϕ dependent curvature bias with specially treated and weighted $Z^0 \to \mu^+\mu^-$ events, the alignment framework extended to treat also calibration parameters, and Lorentz angle calibration integrated into alignment.

Most of these improvements were in full use already in 2012. When LHC operation begins

again in 2015, these improvements will be needed to handle the challenges of the new regime of high luminosity, where for instance time-dependent changes of the Lorentz angle can be expected.

Acknowledgments
The CMS Tracker Alignment group, the Helmholtz Alliance "Physics at the Terascale", the Magnus Ehrnrooth Foundation, and the Waldemar von Frenckell Foundation are acknowledged.

References
[1] CMS Collaboration 2008 *JINST* **3** S08004
[2] CMS Collaboration 2010 *JINST* **5** T03009
[3] Lampén T 2011 Alignment of the CMS silicon tracker, *J. Phys.: Conf. Series* **331** 032043
[4] Draeger J 2010 The alignment of the CMS Silicon Tracker, PoS(ICHEP 2010) **504**
[5] Flucke G 2012 Alignment of the CMS silicon tracker, *J. Phys.: Conf. Series* **368** 012036
[6] Blobel V 2006 Software alignment for tracking detectors, NIM **A566** pp 5-13
[7] https://www.wiki.terascale.de/index.php/Millepede_II
[8] Karimäki V, Heikkinen A, Lampén T and Lindén T 2003 Sensor alignment by tracks, ePrint **physics/0306034** (CMS-CR-2003-022)
[9] Lampén T 2011 CMS silicon strip tracker calibration work-flow and tools , *J. Phys.: Conf. Series* **331** 032044